1 Introduction

2 Preliminaries

2.1 Simplicial Lattice

A simplicial lattice is characterized by multi-indices, $\boldsymbol{\alpha}$, with a length of $n+1$ where each component is a non-negative integer. The degree of a multi-index is the sum of its components. We denote the set of all multi-indices of degree k as $\mathbb{T}_k^n$. Multi-indices can be arranged using the dictionary order, R_n, which depends on the length of the multi-index.

2.2 Interpolation Points

An n-simplex, T, is defined by the convex hull of $n+1$ distinct points. Every point within T can be expressed using barycentric coordinates, $\boldsymbol{\lambda}$. The set $\mathbb{T}_k^n$ of multi-indices can be embedded geometrically into T. Their ordering is described by $R_n(\boldsymbol{\alpha})$. The figure showcases the interpolation points on a triangle for the degree $k = 4$.

2.3 Sub-simplices and Sub-simplicial Lattices

Any simplex, T, encompasses subsimplices across multiple dimensions. $\Delta(T)$ encompasses all subsimplices within T, while $\Delta_\ell(T)$ focuses on those of dimension ℓ. Each sub-simplex has both geometric and algebraic representations. Additionally, for each sub-simplex f, there is a corresponding opposite sub-simplex f^*. The relationship between a multi-index in a sub-simplex and its encompassing simplex is outlined by the prolongation/extension operator, E.

2.4 Bubble Polynomial

The Bernstein representation defines the polynomial space of degree k over a simplex. A sub-simplex, f, has its bubble polynomial, which is of degree $\ell+1$. This bubble polynomial exhibits properties that make it zero on specific subsimplices.

2.5 Triangulation

A geometric triangulation of a polyhedral domain, Ω, in $\mathbb{R}^n$ consists of n-simplices.

3 Geometric Decompositions of Lagrange elements

3.1 Geometric decomposition

For the polynomial space $\mathbb{P}_k(T)$ with $k \geq 1$ on an n-dimensional simplex T, we have the following geometric decomposition of Lagrange element:

Theorem 1 (Geometric decomposition of Lagrange element). *For the polynomial space $\mathbb{P}_k(T)$ with $k \geq 1$ on an n-dimensional simplex T, the decomposition is given by:*

$$\mathbb{P}_k(T) = \bigoplus_{\ell=0}^{n} \bigoplus_{f \in \Delta_\ell(T)} b_f \mathbb{P}_{k-(\ell+1)}(f). \tag{1}$$

Furthermore, the bubble polynomial space of degree k on a sub-simplex f is defined by:

$$\mathbb{B}_k(f) := b_f \mathbb{P}_{k-(\ell+1)}(f).$$

Thus, we can rewrite the decomposition as:

$$\mathbb{P}_k(T) = \mathbb{P}_1(T) \oplus \bigoplus_{\ell=1}^{n} \bigoplus_{f \in \Delta_\ell(T)} \mathbb{B}_k(f). \tag{2}$$

3.2 Lagrange interpolation basis functions

We can represent the DoFs as function values on the interpolation points:

Lemma 1 (Lagrange interpolation basis functions). *A basis function of k-th order Lagrange finite element space on T is given by:*

$$\phi_{\boldsymbol{\alpha}}(\boldsymbol{x}) = \frac{1}{\boldsymbol{\alpha}!} \prod_{i=0}^{n} \prod_{j=0}^{\alpha_i - 1} (k\lambda_i(\boldsymbol{x}) - j),$$

with the DoFs defined as:

$$N_{\boldsymbol{\alpha}}(u) = u(\boldsymbol{x}_\alpha),$$

where $\boldsymbol{x}_\alpha \in \mathcal{X}_T$.

4 Geometric Decompositions of Face Elements

In this section, the geometric decompositions of face elements are expounded upon. The function space $H(div, \Omega)$ comprises vector functions in $L^2(\Omega; \mathbb{R}^n)$ where their divergence is a member of $L^2(\Omega)$. The divergence's trace operator on a subdomain K within Ω projects the vector function to the outward normal on K's boundary.

The section further elaborates on the concept of $H(div)$-conformity, which requires that the normal component of a function is continuous across all the faces of a triangulation $\mathcal{T}_h$. Such conforming elements are also referred to as face elements. Two specific kinds of face elements are introduced: Brezzi-Douglas-Marini (BDM) elements and the second family of Nédélec face elements. These elements have shape functions that span the full polynomial space $\mathbb{P}_k^n$.

4.1 Geometric Decomposition

A new polynomial space known as the divergence bubble space, $\mathbb{B}_k(div; T)$, is introduced, which captures functions that lie in the polynomial space but have a zero trace in terms of divergence. Another significant concept introduced is the tangential bubble polynomials on the tangential plane of a face. It is shown that for $k \geq 2$ and $\dim f \geq 1$, the tangential bubble polynomials are subsets of the divergence bubble space.

A lemma provides the decomposition of the divergence bubble polynomial space as the direct sum of bubble polynomials across different dimensions of sub-simplices within the triangulation.

A key theorem in the section presents two geometric decompositions of a divergence element in terms of polynomial spaces, bubble functions, and normal vectors. The first decomposition singles out the space $\mathbb{P}_1^n(T)$ to highlight the fact that a divergence-conforming element can be constructed by adding divergence bubbles and normal components on sub-simplices starting from edges. The second decomposition groups all the normal components by face, resulting in the classical BDM element.

Lastly, the section stresses the importance of the normal continuity required by $H(div, \Omega)$-conforming elements. This means that the normal vector $\boldsymbol{n}_F$ on a face F is globally defined, but tangential components are multi-valued and local to each face.

4.2 Tangential-normal Decomposition of BDM Element

For a given triangulation $\mathcal{T}_h$, every face $F \in \Delta_{n-1}(\mathcal{T}_h)$ has an associated global normal vector $\boldsymbol{n}_F$. This means that $\boldsymbol{n}_F$ is solely dependent on F and not on the element T containing F.

For every $f \in \Delta_\ell(T)$, the normal basis for its normal plane consists of $\{\boldsymbol{n}_F\}$ where f is a subsimplex of F in ∂T. Additionally, any basis for its tangential plane is considered valid.

The primary assertion made in this subsection is that the resulting element, when constructed in this manner, is equivalent to the BDM element.

A set of Degrees of Freedom (DoFs) is given by

$$\int_f (\boldsymbol{u} \cdot \boldsymbol{n}_F)\, p \,\mathrm{d}s \quad \text{for } F \in \Delta_{n-1}(T) \text{ where } f \subseteq F, \tag{3}$$

$$\int_f (\boldsymbol{u} \cdot \boldsymbol{t}_i^f)\, p \,\mathrm{d}s \quad \text{for } i = 1, \ldots, \ell. \tag{4}$$

For every $p \in \mathbb{P}_{k-(\ell+1)}(f)$ and for all $f \in \Delta_\ell(T)$, $\ell = 0, 1, \ldots, n$.

These DoFs are equivalent to the BDM element represented as:

$$\int_F \boldsymbol{v} \cdot \boldsymbol{n}_F p \,\mathrm{d}S \quad \text{for } p \in \mathbb{P}_k(F) \text{ and } F \in \Delta_{n-1}(T), \tag{5}$$

$$\int_T \boldsymbol{v} \cdot \boldsymbol{p} \,\mathrm{d}x \quad \text{for } \boldsymbol{p} \in \mathbb{B}_k(div; T). \tag{6}$$

The proof for the unisolvence of DoFs follows from Lemma **??** and the redefinition of the basis vectors. Using the geometric decomposition of the Lagrange element and invoking Lemma **??**, we can combine the DoFs as described to yield the equivalent BDM element.

4.3 A basis for the BDM element

The section outlines a modified approach to express the BDM (Brezzi-Douglas-Marini) element using DoFs (Degrees of Freedom) based on function values at interpolation nodes, incorporating the $t-n$ decomposition.

For any $f \in \Delta_\ell(T)$, a basis for its normal plane, $\mathcal{N}^f$, is selected as $\{\boldsymbol{n}_F, F \in \Delta_{n-1}(T), f \subseteq F\}$. Dual bases are constructed for both the normal plane, using the orthogonality relations and for the tangential plane. Specifically, for the normal plane, a dual basis $\{\hat{\boldsymbol{n}}_F\}$ is introduced, satisfying orthogonality conditions with the primary basis $\{\boldsymbol{n}_F\}$. Lemma **??** provides an explicit expression for the dual basis $\hat{\boldsymbol{n}}_{F_i}$.

Moreover, given an interpolation point $\boldsymbol{x} \in \mathcal{X}_T$, both a primary and dual basis for the tangential and normal planes are combined, leading to

$\{\boldsymbol{e}_{\boldsymbol{x}}^i, i = 0, \dots, n-1\}$ and its dual counterpart. A key result states that any polynomial function $\boldsymbol{u} \in \mathbb{P}_k^n(T)$ can be uniquely determined using a specific set of DoFs, and a basis function for the BDM element space is explicitly described.

The novel aspect of this approach is the utilization of a basis from the well-known Lagrange element, coupled with varied $t-n$ decomposition for different sub-simplices, to achieve the BDM element. The section further clarifies that by choosing a global normal basis, continuity is imposed on the normal direction, while no continuity is required in the tangential direction by using a local $\boldsymbol{t}^f$.

Finally, the framework for BDM elements on triangular meshes is presented. Depending on the position of the interpolation point, $\boldsymbol{x}$, within the triangle T, different frames ($\{\boldsymbol{e}_{\boldsymbol{x}}^0, \boldsymbol{e}_{\boldsymbol{x}}^1\}$ and their duals) are chosen, providing a basis that adheres to specific geometric considerations. A visual representation illustrates these bases at each interpolation point.

Given a tetrahedron T and an interpolation point $\boldsymbol{x} \in \mathcal{X}_T$, frames $\boldsymbol{e}_{\boldsymbol{x}}^0, \boldsymbol{e}_{\boldsymbol{x}}^1, \boldsymbol{e}_{\boldsymbol{x}}^2\}$ and their dual frames $\{\hat{\boldsymbol{e}}_{\boldsymbol{x}}^0, \hat{\boldsymbol{e}}_{\boldsymbol{x}}^1, \hat{\boldsymbol{e}}_{\boldsymbol{x}}^2\}$ are chosen based on the position of $\boldsymbol{x}$

1. **Vertex Case:**
   For $\boldsymbol{x} \in \Delta_0(T)$ (a vertex), with adjacent edges e_0, e_1, e_2 and faces F_0, F_1, F_2 such that $F_i \cap e_i = \boldsymbol{x}$, frames are set based on the normal vectors of the adjacent faces and their relationship with the tangent vectors of the adjacent edges.

2. **Edge Interior Case:**
   For $\boldsymbol{x} \in \mathcal{X}_{\mathring{e}}$, $e \in \Delta_1(T)$ (inside an edge), with adjacent faces F_0 and F_1, frames are set based on the normal vectors of the adjacent faces, the edge's tangent vector, and their cross products.

3. **Face Interior Case:**
   For $\boldsymbol{x} \in \mathcal{X}_{\mathring{F}}$ with $F \in \Delta_2(T), e \in \partial F$ (inside a face), frames are set based on the face's normal vector and the edge's tangent vector and their cross product.

4. **Tetrahedron Interior Case:**
   For $\boldsymbol{x} \in \mathcal{X}_{\mathring{T}}$ (inside the tetrahedron), canonical basis vectors are used as the frames.

Illustration: Two figures illustrate these frame definitions. The left figure presents the vectors $\{\boldsymbol{e}_0, \boldsymbol{e}_1, \boldsymbol{e}_2\}$ at each interpolation point, while the right figure showcases the dual vectors $\{\hat{\boldsymbol{e}}_0, \hat{\boldsymbol{e}}_1, \hat{\boldsymbol{e}}_2\}$ at these points.

5 Geometric Decompositions of Edge elements

In this section, we highlight the geometric decompositions for $H(\operatorname{curl})$-conforming finite element space on simplex grids. The presentation hinges on a set of mathematical definitions, notations, and results.

5.1 Essential Concepts and Definitions

- **Differential Operators:** The curl of a vector function $\boldsymbol{v}$ is defined as the skew part of its gradient, which results in a skew-symmetric matrix function. The curl is represented differently in two and three dimensions. In 2D, it is a scalar whereas in 3D, it takes the form of a vector.

- **Sobolev Space:** The Sobolev space associated with the curl, denoted by $H(\operatorname{curl}, \Omega)$, consists of vector functions for which the curl is square-integrable.

- **Trace Operator of Curl:** For a given face F of a tetrahedron T, the trace operator of the curl, termed $\operatorname{tr}_F^{\operatorname{curl}} \boldsymbol{v}$, is a matrix, capturing the relationship between the vector and the normal to the face. The tangential component of $\boldsymbol{v}$, however, remains a vector.

5.2 Key Results

- **Relationship between Tangential Part and Tangential Trace:** The tangential component of $\boldsymbol{v}$ can be represented using its trace, which has been proven with a lemma. Essentially, if the tangential trace vanishes, so does the tangential part.

- **Characterization of $H(\operatorname{curl}, \Omega)$ Elements:** For vector functions that are square-integrable over Ω and have symmetric gradients within each tetrahedron T, such functions belong to $H(\operatorname{curl}, \Omega)$ only if their tangential components match on every shared face between two neighboring tetrahedra.

5.3 Geometric decompositions

A polynomial bubble space for the curl operator is defined as

$$\mathbb{B}_k(\operatorname{curl}, T) = \ker(\operatorname{tr}^{\operatorname{curl}}) \cap \mathbb{P}_k^n(T).$$

For Lagrange bubble $\mathbb{B}_k^n(T)$, components vanish on ∂T and sub-simplex with dimension $\leq n-1$. For vectors in $\mathbb{B}_k(\operatorname{curl};T)$, only tangential components vanish on sub-simplex with dimension $\leq n-2$.

A lemma proves that for any vector in $\mathbb{B}_k(\operatorname{curl},T)$, it's zero on every face f in the set $\Delta_\ell(T)$ where $0 \leq \ell \leq n-2$. This confirms a certain inclusion relationship for $\mathbb{B}_k(\operatorname{curl},T)$.

Furthermore, it's clear that $\mathbb{B}_k^n(T)$ is a subset of $\mathbb{B}_k(\operatorname{curl},T)$. The theorem then claims that the polynomial bubble space decomposes into two primary components: one associated with the original polynomial bubble space and another with normal components on faces of the simplex.

Additionally, the curl operator is restricted to sub-simplices of dimension greater than or equal to 2. The curl-bubble function doesn't include edges, and this results in certain modifications when $\ell = 1$.

In conclusion, two main theorems break down the vector polynomial space into constituent parts: one theorem offers a decomposition based on edges and sub-simplex, while the second offers a more specific decomposition.

5.4 Tangential-Normal decomposition of second family of Nédélec element

Theorem 2. *Given the shape function space $\mathbb{P}_k(T;\mathbb{R}^n)$ and an edge $e \in \Delta_{\ell-1}(T)$, a basis for the normal plane $\mathscr{N}^e$ is given by $\{\boldsymbol{n}_{f,e}, e \subseteq f \in \Delta_\ell(T)\}$ and a basis of $\mathscr{T}^e$ by $\{\boldsymbol{t}_i^f\}$. The Degrees of Freedom (DoFs) for $\ell = 1, \ldots, n$, as given in* (**??**)*, are equivalent to the Nédélec element* (**??**)*.*

The equivalence of DoFs in (**??**) for $\mathbb{P}_k(T;\mathbb{R}^n)$ is justified based on Lemma **??** and by modifying the basis of normal planes. By rearranging the edge e and face f, the DoFs (**??**) can be expressed as (**??**) for $f \in \Delta_\ell(T), \ell = 2, \ldots, n$. Using (**??**) and (**??**), the DoFs in (**??**) are equivalent to DoFs in (**??**).

For an edge $e \in \Delta_{\ell-1}(T)$, there's a redistribution of the normal DoFs (**??**) on e to the tangential part (**??**) of a face f such that $e \subseteq f \in \Delta_\ell(T)$.

Remark 3. *The DoFs for the second kind Nédélec element as referenced in [**?**, **?**] are provided.*

5.5 A basis for the Nédélec element

5.5.1 Nédélec element on triangular meshes

For a triangle T and lattice point $\boldsymbol{x}$ situated in various sub-simplices, distinct frames $\{\boldsymbol{e}_{\boldsymbol{x}}^0, \boldsymbol{e}_{\boldsymbol{x}}^1\}$ and their dual frames $\{\hat{\boldsymbol{e}}_{\boldsymbol{x}}^0, \hat{\boldsymbol{e}}_{\boldsymbol{x}}^1\}$ are chosen. The frames are based on the location of $\boldsymbol{x}$ and are associated with tangential and normal vectors of the triangle edges.

For any $\boldsymbol{u} \in \mathbb{P}_k^2(T)$, it can be uniquely described using degrees of freedom (DoFs) $N_{\boldsymbol{\alpha}}^i(\boldsymbol{u})$. The kth order second type Nédélec element space on T has a basis function defined as $\boldsymbol{\phi}_{\boldsymbol{\alpha}}^i(\boldsymbol{x})$.

Given a conforming triangulation $\mathcal{T}_h$ with edge e, global tangential vectors $\boldsymbol{t}_e$, and local outwards normal vectors $\boldsymbol{n}_e(T)$ are chosen. Several DoFs, associated with edges and cells, help define an $H(\text{curl})$-conforming space V_h.

5.5.2 Nédélec element on tetrahedron meshes

For a tetrahedron T and any point $\boldsymbol{x} \in \mathcal{X}_T$, a frame $\{\boldsymbol{e}_{\boldsymbol{x}}^0, \boldsymbol{e}_{\boldsymbol{x}}^1, \boldsymbol{e}_{\boldsymbol{x}}^2\}$ and its dual frame $\{\hat{\boldsymbol{e}}_{\boldsymbol{x}}^0, \hat{\boldsymbol{e}}_{\boldsymbol{x}}^1, \hat{\boldsymbol{e}}_{\boldsymbol{x}}^2\}$ are established. These frames depend on the location of $\boldsymbol{x}$ and relate to the tangential vectors and normals of the tetrahedron's edges and faces.

6 Management of Global DoFs

This section elaborates on the transition from local to global Degrees of Freedom (DoFs). Within an element, the dictionary indexing of interpolation points is discussed in Section **??**. The assembly of local matrices requires an understanding of mapping from local to global DoFs. Such mapping is straightforward for certain face elements due to normal continuity, but can be multifaceted for element-wise DoFs. The main focus is on the global indexing rules for different finite element spaces: Lagrange, BDM, and Nédélec.

6.1 Lagrange finite element space

Using the tetrahedral mesh as an exemplar, the section illustrates the indexing problem. The local ordering of the tetrahedron's vertices adheres to the right-hand rule, while the interpolation points conform to a dictionary ordering map. Due to the continuity of the Lagrange element, boundary interpolation points require a global index. The data structure of the tetrahedral mesh is given by quantities such as `NN`, `NE`, `NF`, and `NC`, representing numbers of nodes, edges, faces, and cells respectively. Arrays like `node`, `cell`, `SEdge`, `SFace`, and `OFace` help represent the mesh and define the local edges and faces.

The task of indexing the interpolation points on the tetrahedral mesh is then defined mathematically using variables such as k, the degree of the

Lagrange finite element space. Interpolation points that match with the vertices get global indices from 0 to $\texttt{NN} - 1$. For higher degrees ($k > 1$), the global indices for interpolation points inside edges and faces are systematically assigned.

The challenge lies in indexing interpolation points inside an edge or a face as they can be shared by multiple elements. The procedure involves dictionary ordering to compute the local face index j, and subsequently obtaining two representations of the face: local (`LFace`) and global (`GFace`). Argument sorting ensures correct alignment of interpolation points to the global representation.

6.2 BDM and Nédélec finite element space

BDM and Nédélec finite element spaces focus on managing the continuity through the Degree of Freedoms (DoFs) of vector type by establishing a vector frame at each interpolation point. These vector spaces combine the Lagrange basis function with the dual frame of the DoFs to define their vector basis functions. Each DoF in these spaces can be related to a unique interpolation point p and a vector $\boldsymbol{e}$, and each basis function can similarly be associated with a unique Lagrange basis function on p and a dual vector $\boldsymbol{e}'$ of $\boldsymbol{e}$.

The essence of managing DoFs is counting. Initially, we have to lay down global and local indexing rules. Globally, DoFs can be categorized as shared and unshared among simplexes, with shared ones further divided based on their location on edges or faces. Importantly, BDM and Nédélec spaces have no shared DoFs on nodes, and the 3D BDM space lacks DoFs shared on edges. Thus, the global numbering aligns with the Lagrange interpolation points' sequence. An array named `dof2vector` can be deduced from this global rule, storing the vector for each DoF.

Locally, the rule leads to another array `cell2dof` that relates each cell to its DoFs. A unique local index is defined for each DoF based on its interpolation point and its vector within the frame of that point. The `cell2dof` array, considering the interpolation point's location and the global rule, can then be computed.

Remark 4. *The local and global numbering conventions discussed aren't the only possibilities. Moreover, the `cell2dof` array ensures that the higher-order finite element methods discussed in this text have a matrix vector assembly and boundary condition handling process similar to conventional finite element methods.*

7 Numerical Examples

We numerically verify the 3-dimensional BDM elements basis and the second kind of Nédélec element basis using two test problems over the domain $\Omega = (0,1)^3$ partitioned into a structured tetrahedron mesh $\mathcal{T}$, as displayed in Fig **??**.

7.1 High Order Elements for Maxwell Equations

The time harmonic problem is presented, where the variational formulation involves the curl operation on the electric field vector $\boldsymbol{E}$. We utilize the second Nédélec space with degree k on $\mathcal{T}$ to approximate the solution. Choosing specific functions for $\boldsymbol{E}$ and $\boldsymbol{J}$, our numerical results (Fig **??**) suggest that the approximation error in $\boldsymbol{E}$ is of order $O(h^{k+1})$ and the error in its curl is of order $O(h^k)$.

7.2 High Order Elements for Mixed Poisson

The mixed Poisson problem is described, where the variational formulation involves the divergence operation on the vector $\boldsymbol{u}$ and the pressure field p. We use the BDM space with degree k on $\mathcal{T}$ and a piecewise polynomial space of degree $k-1$ to approximate the solution. Adopting specific functions for $\boldsymbol{u}$ and p, our numerical results (Fig **??**) show that the approximation error in $\boldsymbol{u}$ is of order $O(h^{k+1})$ and the error in p is of order $O(h^k)$.

8 Management of Global DoFs

In Section **??**, we introduced the dictionary indexing mechanism for interpolation points within each element. Based on these interpolation points, matrices can be computed for each element. During the assembly of these local matrices, it becomes essential to understand the mapping from local DoFs to global DoFs. Consider face elements: due to the normal continuity, the face DoFs are single-valued, and their index is global, irrespective of the element. Conversely, element-wise DoFs are local and have multiple values, exemplified by the tangential $H(\mathrm{div})$-bubble DoFs given by Equations (**??**) and (**??**). The core of implementing a finite element algorithm lies in efficiently managing the mapping from local to global DoFs. This section elucidates the global indexing rules for Lagrange, BDM, and Nédélec finite element spaces.

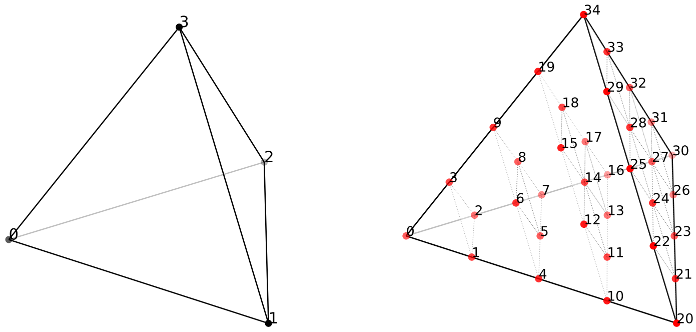

Figure 1: Indexing rules for the vertices of a tetrahedron and interpolation points with $k = 4$ on it.

8.1 Lagrange finite element space

Using the tetrahedral mesh as an illustrative example, Figure 1 displays the local indexing rules for the tetrahedron's vertices and the interpolation points when $k = 4$. The tetrahedron's four vertices are ordered according to the right-hand rule, and the interpolation points adhere to the dictionary ordering map $R_3(\boldsymbol{\alpha})$. Since the Lagrange element is continuous, interpolation points on the boundary ∂T must have a global index. Thus, a unique index is required for points on vertices, edges, and faces, along with a mapping from local to global indices.

We begin by discussing the data structure of the tetrahedral mesh, denoted by $\mathcal{T}_h$. Let the numbers of nodes, edges, faces, and cells in $\mathcal{T}_h$ be represented as `NN`, `NE`, `NF`, and `NC`, respectively. We utilize two arrays to represent $\mathcal{T}_h$:

- `node` (shape: `(NN,3)`): `node[i,j]` represents the j-th component of the Cartesian coordinate of the i-th vertex.

- `cell` (shape: `(NC,4)`): `cell[i,j]` gives the global index of the j-th vertex of the i-th cell.

Given a tetrahedron denoted by `[0,1,2,3]`, we define its local edges and faces as:

- `SEdge = [(0,1),(0,2),(0,3),(1,2),(1,3),(2,3)];`

- `SFace = [(1,2,3),(0,2,3),(0,1,3),(0,1,2)];`

- `OFace = [(1,2,3),(0,3,2),(0,1,3),(0,2,1)];`

Here, we introduced two types of local faces. The prefix `S` implies sorting, and `O` indicates outer normal direction. Both `SFace[i,:]` and `OFace[i,:]` represent the face opposite to the i-th vertex but with varied ordering. The normal direction as determined by the ordering of the three vertices of `OFace` matches the outer normal direction of the tetrahedron. This ensures that the outer normal direction of a boundary `face` points outward from the mesh. Meanwhile, `SFace` aids in determining the global index of the interpolation points on the face. For an in-depth discourse on indexing, ordering, and orientation, we direct readers to `sc3` in iFEM [**?**].

Leveraging the `unique` algorithm for arrays, we can derive the following arrays from `cell`, `SEdge`, and `OFace`:

- `edge` (shape: `(NE,2)`): `edge[i,j]` gives the global index of the j-th vertex of the i-th edge.
- `face` (shape: `(NF,3)`): `face[i,j]` provides the global index of the j-th vertex of the i-th face.
- `cell2edge` (shape: `(NC,6)`): `cell2edge[i,j]` indicates the global index of the j-th edge of the i-th cell.
- `cell2face` (shape: `(NC,4)`): `cell2face[i,j]` signifies the global index of the j-th face of the i-th cell.

Having constructed the edge and face arrays and linked cells to them, we next establish indexing rules for interpolation points on $\mathcal{T}_h$. Let k be the degree of the Lagrange finite element space. The number of interpolation points on each cell is

$$\mathtt{ldof} = \dim \mathbb{P}_k(T) = \frac{(k+1)(k+2)(k+3)}{6},$$

and the total number on $\mathcal{T}_h$ is

$$\mathtt{gdof} = \mathtt{NN} + n_e^k \cdot \mathtt{NE} + n_f^k \cdot \mathtt{NF} + n_c^k \cdot \mathtt{NC},$$

where

$$n_e^k = k-1, \quad n_f^k = \frac{(k-2)(k-1)}{2}, \quad n_c^k = \frac{(k-3)(k-2)(k-1)}{6}.$$

The global index of interpolation points on a face can be obtained via `SFace`, and the local index is derived from the dictionary ordering map $R_2(\boldsymbol{\alpha})$ for $0 \le \alpha_i \le k$. This mapping guarantees that interpolation points on a face shared by two cells have the same global index. Additionally, the global index of interpolation points inside a cell is determined by the dictionary ordering map $R_3(\boldsymbol{\alpha})$.

In essence, establishing these rules facilitates the efficient assembly of global matrices and vectors, which is crucial for computational efficiency. Detailed algorithms are discussed in [**?**].

8.2 Constructing the `cell2ipoint` Array

The two-dimensional array named `cell2ipoint` of shape `(NC,ldof)` is crucial in our discussion. For the j-th interpolation point of the i-th cell, we aim to determine its unique global index and store it in `cell2ipoint[i,j]`.

The combination of the simplicial lattices set $\mathbb{T}_k^n$ and the ordering map $R(\boldsymbol{\alpha})$ readily informs the position of each interpolation point relative to the simplex and its sub-simplexes. If the j-th interpolation point either coincides with a vertex or is situated inside a cell, the global indexing rule previously discussed simplifies the assignment of `cell2ipoint[i,j]`. However, complications arise when the interpolation point is located within an edge or face since these elements can be shared by multiple cells.

Consider, for instance, the scenario where the j-th interpolation point lies within the 0-th local face F_0 of the i-th cell. Let $\alpha =$ `m = [m0,m1,m2,m3]` be its lattice point. Given that F_0 is opposite to vertex 0, we deduce that $\lambda_0|_{F_0} = 0$, which implies `m0` is 0. The remaining components of $\boldsymbol{m}$ are non-zero, ensuring that the point is interior to F_0. Using the dictionary ordering, we express j as:

$$
\begin{aligned}
j =& \frac{(\mathtt{m1}+\mathtt{m2}+\mathtt{m3})(\mathtt{m1}+\mathtt{m2}+\mathtt{m3}+1)(\mathtt{m1}+\mathtt{m2}+\mathtt{m3}+2)}{6} \\
&+ \frac{(\mathtt{m2}+\mathtt{m3})(\mathtt{m2}+\mathtt{m3}+1)}{2} + \mathtt{m3}.
\end{aligned}
$$

Two representations for the face with global index `cell2face[i,0]` are subsequently acquired:

- `LFace = cell[i,SFace[0,:]]` (local representation)
- `GFace = face[cell2face[i,0],:]` (global representation)

Although `LFace` and `GFace` comprise identical vertex numbers, their ordering differs. The array `m = [m1,m2,m3]` has a one-to-one correspondence with the vertices of `LFace`. To match this array with the vertices of `GFace`, a reordering based on argument sorting is performed:

```
i0 = argsort(argsort(GFace));
i1 = argsort(LFace);
i2 = i1[i0];
m = m[i2]}.
```

From the reordered `m = [m1,m2,m3]`, the local index ℓ of the j-th interpolation point on the global face `f = cell2face[i,0]` can be deduced:

$$\begin{aligned}\ell =&\frac{(\mathtt{m2}-1+\mathtt{m3}-1)(\mathtt{m2}-1+\mathtt{m3}-1+1)}{2}+\mathtt{m3}-1\\ =&\frac{(\mathtt{m2}+\mathtt{m3}-2)(\mathtt{m2}+\mathtt{m3}-1)}{2}+\mathtt{m3}-1.\end{aligned}$$

It's worth noting that the index of interpolation points solely within the face needs consideration. Finally, the global index J for the j-th interpolation point within the 0-th local face of the i-th cell is:

$$J = \mathtt{NN} + n_e^k \cdot \mathtt{NE} + n_f^k \cdot \mathtt{NF} + \ell.$$

In conclusion, we've elucidated the construction of global indexing for interpolation points inside cell faces. This method can be generalized for edges and, more broadly, for interior interpolation points of the low-dimensional sub-simplex of an n-dimensional simplex.